






# In vivo pulsed-field ablation in healthy vs. chronically infarcted ventricular myocardium: biophysical and histologic characterization

Uday Sandhu <sup>1</sup>, Laith Alkukhun<sup>1</sup>, Babikir Kheiri <sup>1</sup>, James Hodovan <sup>1</sup>, Kirby Chiang<sup>2</sup>, Taylor Splanger<sup>3</sup>, Quim Castellvi <sup>2</sup>, Yan Zhao<sup>1</sup>, and Babak Nazer <sup>1</sup>\*

<sup>1</sup>Knight Cardiovascular Institute, Oregon Health and Science University, 3181 SW Sam Jackson Park Road, Portland, OR 97239, USA; <sup>2</sup>Galaxy Medical, 1531 Industrial Road, San Carlos, CA 94070, USA; and <sup>3</sup>VDx Veterinary Diagnostics and Preclinical Research Services, 215 C St #301, Davis, CA 95616, USA

Received 11 August 2022; accepted after revision 11 November 2022; online publish-ahead-of-print 16 February 2023

## Aims

Data on ventricular pulsed-field ablation (PFA) are sparse in the setting of chronic myocardial infarction (MI). The objective of this study was to compare the biophysical and histopathologic characteristics of PFA in healthy and MI swine ventricular myocardium.

## Methods and results

Myocardial infarction swine ( $n = 8$ ) underwent coronary balloon occlusion and survived for 30 days. We then performed endocardial unipolar, biphasic PFA of the MI border zone and a dense scar with electroanatomic mapping and using an irrigated contact force (CF)-sensing catheter with the CENTAURI System (Galaxy Medical). Lesion and biophysical characteristics were compared with three controls: MI swine undergoing thermal ablation, MI swine undergoing no ablation, and healthy swine undergoing similar PFA applications that included linear lesion sets. Tissues were systematically assessed by gross pathology utilizing 2,3,5-triphenyl-2H-tetrazolium chloride staining and histologically with haematoxylin and eosin and trichrome. Pulsed-field ablation in healthy myocardium generated well-demarcated ellipsoid lesions ( $7.2 \pm 2.1$  mm depth) with contraction band necrosis and myocytolysis. Pulsed-field ablation in MI demonstrated slightly smaller lesions (depth  $5.3 \pm 1.9$  mm,  $P = 0.0002$ ), and lesions infiltrated into the irregular scar border, resulting in contraction band necrosis and myocytolysis of surviving myocytes and extending to the epicardial border of the scar. Coagulative necrosis was present in 75% of thermal ablation controls but only in 16% of PFA lesions. Linear PFA resulted in contiguous linear lesions with no gaps in gross pathology. Neither CF nor local R-wave amplitude reduction correlated with lesion size.

## Conclusion

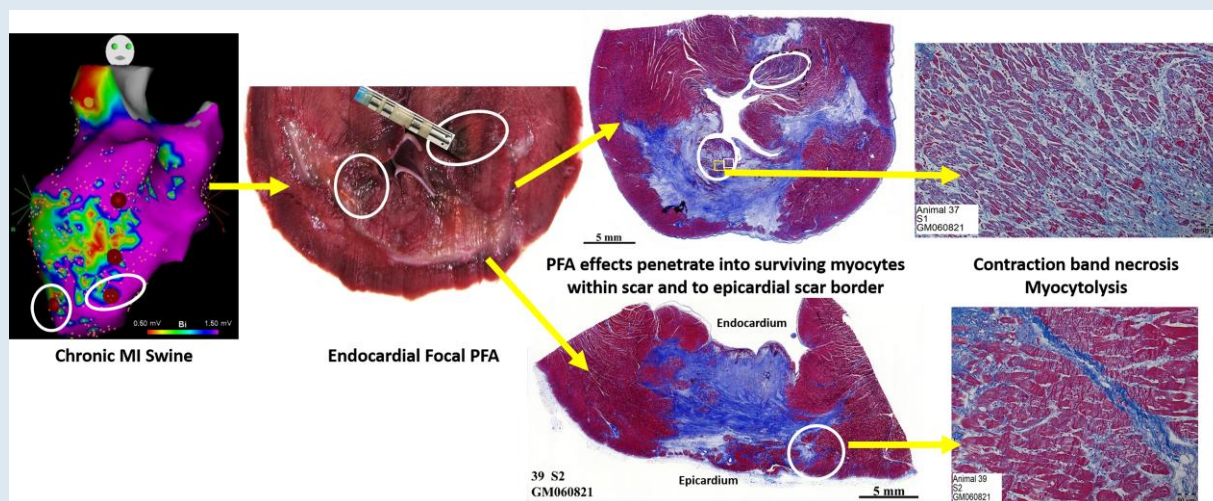
Pulsed-field ablation of a heterogeneous chronic MI scar effectively ablates surviving myocytes within and beyond the scar, demonstrating promise for the clinical ablation of scar-mediated ventricular arrhythmias.

\* Corresponding author. Tel: +1 206 598 8074. E-mail address: bnazer@uw.edu

© The Author(s) 2023. Published by Oxford University Press on behalf of the European Society of Cardiology.

This is an Open Access article distributed under the terms of the Creative Commons Attribution-NonCommercial License (<https://creativecommons.org/licenses/by-nc/4.0/>), which permits non-commercial re-use, distribution, and reproduction in any medium, provided the original work is properly cited. For commercial re-use, please contact [journals.permissions@oup.com](mailto:journals.permissions@oup.com)

## Graphical Abstract



## Keywords

Ventricular tachycardia • Ventricular arrhythmia • Pulsed-field ablation • Catheter ablation

## What's new?

- Pulsed-field ablation (PFA) was able to generate effective lesions in and around a ventricular scar in a swine myocardial infarction (MI) model, with lesions that were only slightly smaller than those made in normal myocardium.
- Histology confirmed the penetration of PFA effects into surviving myocytes within the MI scar, and occasionally beyond it, to the epicardial scar border as well.
- Contact force and the degree of R-wave amplitude reduction did not predict lesion formation or lesion size.

## Introduction

Pulsed-field ablation (PFA) is an emerging technology in the field of catheter ablation for cardiac arrhythmias.<sup>1,2</sup> It is a non-thermal mode of ablation unlike radiofrequency (RF) and cryotherapy with tissue specificity. The electric fields disrupt the cellular membrane permeability and haemostasis, alter local tissue pH, and create reactive oxygen species, which can lead to cell death.<sup>1</sup> Early animal data have demonstrated the sparing of coronary vessels, oesophagus, and nerves with no pulmonary vein (PV) stenosis while delivering fast, deep lesions.<sup>2</sup> More recently, this technology has been applied to the treatment of paroxysmal and persistent atrial fibrillation (AF) with PV isolation, posterior wall isolation, and cavo-tricuspid isthmus ablation demonstrated in single-armed trials.<sup>3,4</sup> A 1-year follow-up in paroxysmal AF patients demonstrated  $79.3 \pm 4.6\%$  AF/atrial tachycardia/atrial flutter recurrence exemplifying lesion durability via PFA as well rapid lesion formation with shorter procedure times.<sup>4</sup> Although atrial PFA has proceeded to human randomized trials, there are still sparse data on ventricular muscle ablation with PFA, especially in infarcted myocardium.<sup>5-7</sup> Koruth et al.<sup>5</sup> have demonstrated the use of PFA to create well-demarcated homogenous chronic lesions (35.5 days) in ventricular swine myocardium and even transmural lesions in the right ventricle (RV) with no histological damage to surrounding nerves or arterioles.

In addition, other groups have demonstrated the dose-dependent effect of PFA on epicardial left ventricular (LV) lesions and functional effects on His–Purkinje fibres.<sup>6,7</sup> Repeated PFA application at the same ventricular site appears to increase both lesion depth and width, with consistent results at mean 23 days of post-ablation follow-up where lesions demonstrated fibro-fatty replacement and wall thinning.<sup>8</sup>

However, all the aforementioned studies investigated PFA in healthy myocardium, which may not be relevant to the treatment of scar-based ventricular arrhythmias. It is well described that RF ablation in/around a large animal chronic myocardial infarction (MI) scar generates lesions with ill-defined borders and inconsistent necrosis of surviving myocytes within the scar.<sup>9</sup> Given the distinct ablation mechanisms of PFA, we aimed to assess the biophysical performance and tissue selectivity of ventricular PFA in/around chronic MI scar.

## Methods

## Myocardial infarction model

Eight female farm swine (*sus domesticus*) (40–45 kg) were anaesthetized with tiletamine and zolazepam and intubated. Anaesthesia was maintained with inhaled isoflurane (1.5–3.5% via 2 L/min O<sub>2</sub>). Isothermia was maintained with water-heated blankets. Percutaneous ultrasound-guided femoral arterial access was obtained, and a 7 Fr Hockey Stick guide catheter was used to cannulate the left main coronary artery. Next, a non-compliant angioplasty balloon was advanced to the middle portion of either the left circumflex (LCx) or left anterior descending (LAD) coronary artery and inflated for 90 min. After recovery, swine was survived for 30 days as described previously.<sup>10,11</sup>

## Electroanatomic mapping and pulsed-field ablation

For the terminal mapping and ablation studies, eight post-MI and eight healthy control swine (50–55 kg) underwent general anaesthesia and percutaneous femoral venous and arterial access as described above. Heparin was administered intravenously targeting an activated clotting time of 300–350 s. Carto (Biosense Webster, Irvine, CA, USA)

electroanatomic mapping system was employed with mapping of the RV performed from a femoral venous approach, and of the LV from a retrograde aortic approach using a Pentaray catheter (Biosense Webster; Irvine, CA, USA). In the MI swine, areas of dense scar were defined as  $<0.5$  mV,  $0.5$ – $1.5$  mV as border zone (BZ), and  $>1.5$  mV as healthy tissue. Endocardial ablation was performed using a 3.5 mm irrigated, contact force (CF)-sensing catheter (ThermoCool ST, Biosense Webster, Irvine, CA, USA) connected to the CENTAURI PFA generator (Galaxy Medical, San Carlos, CA, USA) which delivered eight electrocardiogram-gated packets of 25 A of monopolar, biphasic, pulsed fields (WAVE1 waveform). Contact force and local R-wave amplitude from the ablation catheter were measured pre- and immediately post-ablation. In MI swine, ablation was performed in areas of healthy myocardium and dense scar, but preferentially over BZ to be most clinically relevant. Pulsed-field ablation applications were spaced  $>1$  cm apart to allow identification of gross pathology and histology. Healthy swine also underwent linear PFA ablation using the same PFA parameters to create contiguous linear lesion sets using 4 mm diameter marks on the mapping system. All studies were approved and monitored by the Oregon Health & Science University Institutional Animal Care and Use Committee under guidelines set forth by the Association for the Assessment and Accreditation of Laboratory Animal Care, and consistent with the Guide for the Care and Use of Laboratory Animals.

## Control studies

In addition to PFA in healthy myocardium serving as a control, one MI swine underwent no ablation whatsoever, serving as a control for pathologic assessment of expected post-MI myocyte and scar morphology. To distinguish PFA from exclusively thermal ablation effects, MI swine underwent high-intensity ultrasound ablation (30 acoustic W, 60 s) as previously described,<sup>12</sup> which has a known thermal mechanism.<sup>12,13</sup>

## Gross pathology and histology

After a 120 min waiting period from the last ablation to allow PFA lesion maturation, animals were euthanized and tissues simultaneously stained with an intravenous injection of 10 g 2,3,5-triphenyl-2H-tetrazolium chloride in 50 mL saline. Hearts were fixed in 10% formalin at 4°C for 1 week and then sectioned in 4–5 mm thick short-axis segments to allow gross pathologic identification of lesions, taking care to extend apical and basal to the MI scar border and correlating all grossly identifiable lesions with lesion location tags on the electroanatomic map. Lesion depth was measured manually using callipers starting from and orthogonal to the endocardium, and ending at the distal (toward the LV) end of the lesion. Lesion volume was calculated using visual observation of lesion boundaries as input to the revolved ellipsoid volume formula ( $4/3 \times \pi \times D/2 \times W/2 \times T/2$ ), where  $D$  is the lesion depth (measured in the axis going away from the endocardium),  $W$  the width

(along the septal-to-lateral axis), and  $T$  the thickness (along basal-to-apical axis). This equation has been validated for assessment of ablation lesions.<sup>11</sup>

Samples of formalin-fixed heart tissue were trimmed serially through the treatment sites at  $\sim 5$  mm intervals in a short-axis orientation parallel to the atrioventricular groove. Samples for routine paraffin histology were collected from each infarcted serial section, then processed and stained with haematoxylin and eosin. A subset of histology samples were stained with Masson's trichrome at the pathologist's discretion. Each section then underwent systematic histological evaluation by a veterinary pathologist blinded to control/ablation modality. Under both sub-gross and magnified histology, the pathologist evaluated both BZs and the middle of the scar on each short-axis segment. For each section the presence of haemorrhage, interstitial oedema, myocardial contraction bands, myocytolysis (cellular vacuolation), microvascular congestion, and coagulation necrosis (indicative of thermal injury) and denatured collagen (indicative of thermal injury). The severity of each of these changes was graded semi-quantitatively (i.e. from 0 = absent to 4 = severe).

## Statistical analysis

Statistical analysis was performed in GraphPad Prism (San Diego, CA, USA). The relationship between biophysical parameters and lesion sizes was assessed using two-tailed Pearson correlation analysis for continuous variables and two-tailed paired Student's  $t$ -test for dichotomous variables. Comparisons between treatment groups were performed using two-tailed unpaired  $t$ -tests. All values are mean  $\pm$  standard deviation.

## Results

### Healthy myocardium pulsed-field ablation: focal and linear ventricular ablation

For all PFA deliveries, no ventricular fibrillation or other pro-arrhythmia was noted, and there was no gross pathologic evidence of complications including pericardial effusion or cardiac perforation.

Of a total of 58 focal PFA applications, 53 lesions (91% lesion efficiency) were seen on gross pathology of sectioned swine hearts with 44/46 lesions visualized in the LV and 9/12 in the RV. Lesions demonstrated depth of  $6.8 \pm 2.2$  mm with volume  $482 \pm 241$  mm<sup>3</sup> (Figure 1A). Left ventricular lesions were slightly deeper than RV lesions ( $7.2 \pm 2.1$  vs.  $4.6 \pm 0.7$  mm,  $P = 0.0007$ ), but there was no significant difference in volume ( $470 \pm 244$  vs.  $544 \pm 229$  mm<sup>3</sup>,  $P = 0.4$ ). Contact force ranged 7–30 g (mean  $12.7 \pm 4.8$ ;  $13.3 \pm 4.9$  for LV lesions) but there was no significant correlation between CF and lesion depth ( $R^2 = 0.0131$ ) or between CF and lesion volume ( $R^2 = 0.0098$ ; Supplementary material online, Figure S1). Contact force was not a pre-



**Figure 1** Gross pathology of focal (A) and linear (B) PFA. Linear lesion sets made in the anteroseptal LV endocardium (eight PFA applications, 4 cm long) and inferolateral LV endocardium (16 PFA applications, 5.2 cm long) had no visual gaps. LV, left ventricular; PFA, pulsed-field ablation.

specified independent variable in this study but distributed in a clinically relevant manner with 26% of applications achieving 7–9 g, 64% achieving 10–19 g, and 9% achieving 20–30 g. Local R-wave amplitude was  $4.5 \pm 2.4$  mV pre-ablation and reduced to  $2.1 \pm 1.2$  mV post-ablation (53  $\pm$  23% reduction), but there was no significant correlation between R-wave reduction and lesion depth ( $R^2 = 0.0131$ ) or between R-wave reduction and lesion volume ( $R^2 = 0.0079$ ; [Supplementary material online, Figure S2](#)). When healthy myocardium LV lesions were compared between those made in healthy swine vs. chronic MI swine (remote from the infarct tissue), there was no significant difference in depth ( $7.0 \pm 2.2$  vs.  $7.8 \pm 2.4$  mm,  $P = 0.28$ ) or volume ( $448 \pm 247$  vs.  $543 \pm 268$  mm<sup>3</sup>,  $P = 0.28$ ).

Separate from the individual PFA applications, eight linear PFA lesion sets (ranging 6–20 lesions, mean of 13 lesions per line) were made in healthy myocardium. On gross pathology line length ranged 2.4 cm (6 lesion line) to 5.5 cm (20 lesion line) with a mean depth of  $8.3 \pm 2.2$  mm ( $P = 0.38$  for comparison with focal lesion depth). On gross pathology, there were no visual gaps noted along any of the eight lines ([Figure 1B](#)).

### Chronic myocardial infarction pulsed-field ablation: biophysics and gross pathology

Of the eight MI swine, four underwent LCx and four LAD infarcts. The mean scar size (voltage <1.5 mV) was  $34 \pm 15$  cm<sup>2</sup>, comprising  $14 \pm 7\%$  of the endocardial surface area ([Figure 2B](#)).

A total of 89 PFA applications were performed (78 in the BZ and 11 in dense scar), generating 49 lesions (all in BZ; 55% lesion efficiency) that were able to be appreciated on gross pathology. R-wave amplitude reduced from  $1.1 \pm 0.6$  pre-ablation to  $0.7 \pm 0.4$  mV post-ablation (34  $\pm$  22% reduction). When comparing PFA in chronic MI to those performed in healthy LV myocardium ([Table 1](#)), there was no difference

in CF, but lesions in chronic MI had shallower depth ( $5.3 \pm 1.9$  vs.  $7.2 \pm 2.1$  mm,  $P = 0.0002$ ) and lower volume ( $310 \pm 166$  vs.  $470 \pm 244$  mm<sup>3</sup>,  $P = 0.002$ ). Contact force in MI swine ranged 6–35 g with 27% of PFA applications achieving 6–9 g, 44% of achieving 10–19 g, and 11% achieving 20–35 g. We compared the biophysical parameters of PFA applications that resulted in grossly appreciable lesions vs. those that did not, and there was no difference in CF ( $12.6 \pm 5.0$  vs.  $13.7 \pm 6.3$  g,  $P = 0.37$ ), pre-ablation R-wave amplitude ( $1.2 \pm 0.6$  vs.  $0.9 \pm 0.7$  mV,  $P = 0.061$ ) or degree of R-wave amplitude reduction ( $36 \pm 24$  vs.  $33 \pm 22\%$ ,  $P = 0.58$ ). As in healthy myocardium, there was no significant correlation between CF and either lesion depth ( $R^2 = 0.040$ ) or volume ( $R^2 = 0.060$ ), or between R-wave amplitude reduction and lesion depth ( $R^2 = 0.114$ ) or volume ( $R^2 = 0.076$ ).

### Histologic analysis

Pulsed-field ablation lesions in healthy myocardium demonstrated well-demarcated borders with a small core of microhaemorrhage surrounded by contraction band necrosis and myocytolysis (see [Supplementary material online, Figure S3](#)). Pulsed-field ablation lesions at BZ of chronic MI scar similarly demonstrated contraction band necrosis and myocytolysis of surviving myocytes within the scar ([Figures 2 and 3](#)).

Since not all PFA applications of MI swine resulted in a clearly demarcated lesion on gross pathology, we systematically assessed each 3 mm short-axis segment for histologic changes in the mid-dense scar, as well as both BZs (scar edge) and the far-field epicardial border of the scar. A similar analysis was performed for the control MI swine that underwent thermal ablation, and the control MI swine that did not undergo ablation ([Figure 4](#)). In chronic MI PFA swine, contraction band necrosis (100%) and myocytolysis (72%) were common, whereas coagulative necrosis (16%; typically seen with thermal ablation) was rare. Of note, selective contraction bands and myocytolysis of surviving myocytes within chronic MI scar were reproducibly noted ([Figures 2E and F and 3E](#)).

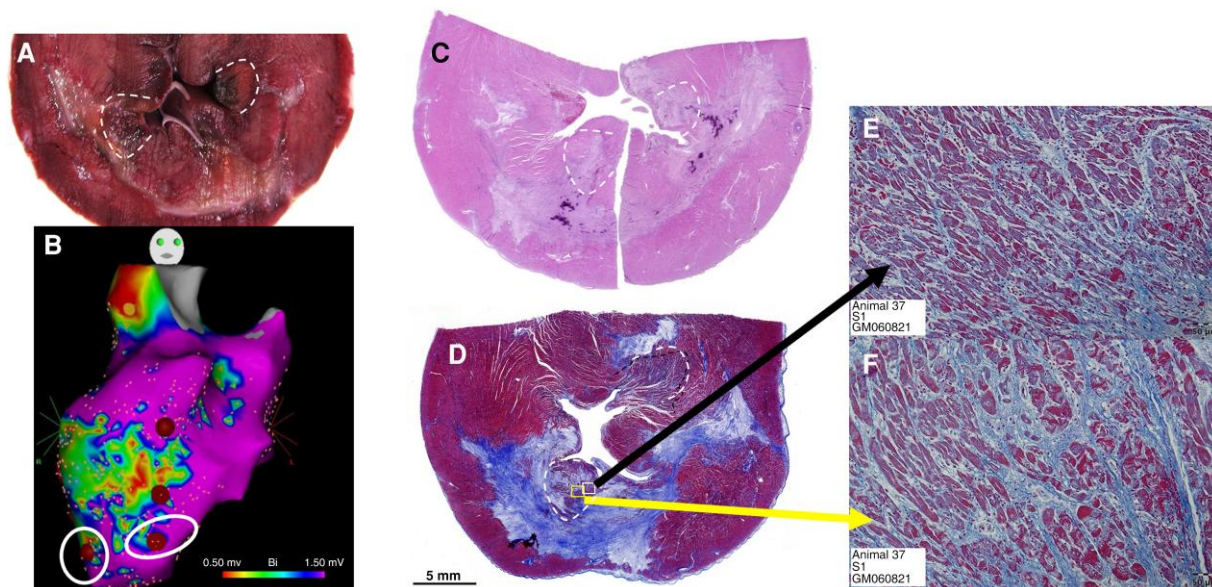


**Figure 2** Pulsed-field ablation of surviving myocytes within chronic subendocardial MI scar. The most apical PFA applications of scar BZ are demonstrated on gross pathology (A), electroanatomic mapping (B), sub-gross pathology with haematoxylin and eosin (C) and trichrome (D), and magnified histology demonstrating contraction band necrosis with oedema of surviving myocytes within scar (E and F). BZ, border zone; MI, myocardial infarction; PFA, pulsed-field ablation.

**Table 1.** PFA lesions in healthy versus chronically infarcted tissue

	Healthy LV myocardium (46 applications, 44 lesions)	Chronic MI (89 applications, 49 lesions)	P-value
Contact force (g)	13.3 ± 4.9	13.1 ± 5.6	0.864
R-wave pre-ablation (mV)	4.5 ± 2.4	1.1 ± 0.6	<0.0001
R-wave post-ablation (mV)	2.1 ± 1.2	0.7 ± 0.4	<0.0001
R-wave reduction (%)	53 ± 23	34 ± 22	0.0002
Depth (mm)	7.2 ± 2.1	5.3 ± 1.9	0.0002
Width (mm)	5.5 ± 1.2	5.1 ± 1.4	0.344
Volume (mm <sup>3</sup> )	470 ± 244	310 ± 166	0.002

LV, left ventricular; MI, myocardial infarction.

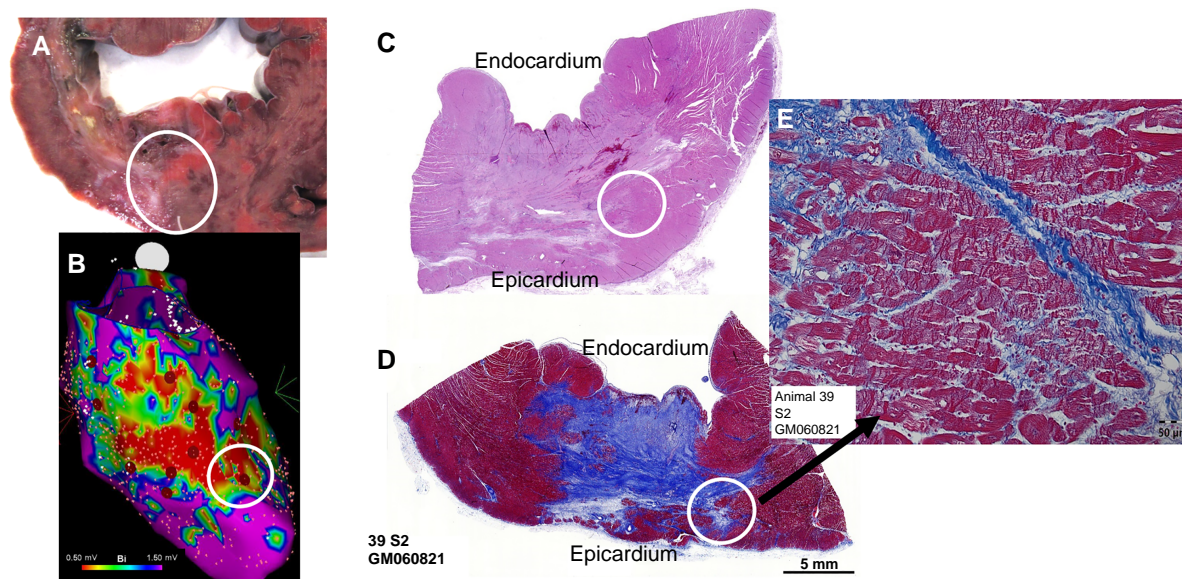


**Figure 3** Pulsed-field ablation extends beyond chronic MI scar to its epicardial border. Pulsed-field ablation application at scar BZ is demonstrated on gross pathology (A), electroanatomic mapping (B), sub-gross pathology with haematoxylin and eosin (C) and trichrome (D), and magnified histology demonstrating contraction band necrosis and myocytolysis extending beyond the scar to its epicardial border (E). BZ, border zone; MI, myocardial infarction.

In the thermally ablated MI swine, all three findings were common (75% demonstrated coagulative necrosis;  $P = 0.01$  for comparison with PFA), whereas none of these types of acute necrosis were present in the non-ablated control MI swine. In a subset of PFA-ablated MI swine, the histologic effects of PFA on a cellular level were noted to extend through the scar and to its epicardial border (Figure 3) in 66% of the MI swine that underwent systematic BZ histologic analysis.

## Discussion

In this study, we demonstrate the ability of unipolar biphasic PFA to generate consistent ventricular lesions in healthy myocardium

(including linear lesions without gaps) using a focal, CF-enabled irrigated catheter without complications. Our lesion depths ( $7.2 \pm 2.1$  mm in LV) were comparable with other pre-clinical ventricular PFA studies reported by Koruth *et al.*<sup>5</sup> ( $6.5 \pm 1.7$  mm), Yavin *et al.*<sup>8</sup> ( $5.6 \pm 1.43$  mm), Neven *et al.*<sup>6</sup> ( $6.3 \pm 1.8$  mm), and Im *et al.*<sup>14</sup> ( $6.1 \pm 1.7$  mm). Furthermore, our ability to generate contiguous linear lesions without gaps by gross pathology using adjacent focal PFA applications further supports PFA's clinical utility for this commonly used strategy for ventricular tachycardia ablation.<sup>15</sup> It should be noted that PFA lesion depth can be increased with increased power (300 J lesions in Neven *et al.* generated depths of  $8.0 \pm 1.5$  mm although this was with a 6 mm electrode inside an epicardial direct-suction device<sup>6</sup>) or with 'stacked,' repeat PFA applications at the same LV site (Yavin *et al.* achieved

Model	Coagulative necrosis (% of sections)	Contraction band necrosis (% of sections)	Myocytolysis (% of sections)
PFA ( <i>n</i> = 25 sections)	16	100	72
Thermal ablation ( <i>n</i> = 4 sections)	75	100	75
No ablation ( <i>n</i> = 6 sections)	0	0	0

**Figure 4** Cellular effects of PFA. Coagulative necrosis (left) was noted much more frequently with thermal ablation than with PFA. Contraction band necrosis and myocytolysis were not noted in chronic MI that was not ablated. PFA, pulsed-field ablation.

$8.8 \pm 0.7$  mm depth with 4 $\times$  repeat PFA applications<sup>8</sup>). We did not perform dose finding in either manner (power or # 'stacked' applications), but it should be noted that neither depth was dramatically deeper than ours of  $7.2 \pm 2.1$  mm in LV. The safety of higher-power PFA (which may begin to incur greater thermal ablation properties) or 'stacked lesions' (which may risk perforation) needs to be further tested.

In our study, there was no correlation between CF and lesion depth or volume, consistent with the notion that high degrees of CF may not be necessary for effective PFA. Other pre-clinical studies have demonstrated a correlation between CF and lesion size,<sup>1,16</sup> but these studies pre-specified CF ranges and included the extremely low CF range (0–10 g), whereas we aimed to achieve >10 g prior to each lesion. Thus, it is likely that the majority of our PFA CF (mean  $13 \pm 5$  g, minimum 7 g) was above the 'plateau threshold' necessary to demonstrate a dose–response effect between CF and lesion size. Furthermore, since CF was not a pre-specified independent variable in our study (we simply aimed to achieve 10–30 g but tolerated lower CF when catheter stability would otherwise be compromised), our conclusions on the relationship between CF and lesion size are exploratory.

Our study also did not demonstrate a correlation between the degree of local R-wave amplitude reduction post-ablation and lesion depth or volume. This relationship has not previously been studied in PFA, but may reflect the fact that acute PFA provides more myocardial 'stunning' due to electroporation, and that the time course to irreversible necrosis may occur over at least 90 min (we re-measured R-wave amplitude immediately post-ablation but did not re-measure prior to euthanasia at 120 min). Local R-wave amplitude reduction is one of several indicators of sufficient ventricular lesion delivery in clinical RF ablation of ventricular arrhythmias but may not be a suitable indicator for ventricular PFA, given this poor correlation and the slower time course of PFA lesion maturation. Thus, additional indicators of satisfactory acute PFA delivery in the ventricle—such as non-capture with high-output pacing or local impedance changes—need to be explored in future studies.

Similar to prior studies of RF ablation in a chronic MI scar,<sup>9</sup> our PFA lesions in and around the scar were not always clearly visualized on gross pathology (especially those made within the dense, middle portion of the scar). However, we were still able to visualize 55% of our

PFA applications compared with only 10% of those seen with RF.<sup>9</sup> Our systematic histology approach was of higher yield than gross pathology in identifying acute PFA changes, which were present at every scar BZ that was analysed. These changes were characterized by contraction band necrosis and myocytolysis of surviving myocytes within the scar, but, unlike the thermally ablated control tissues, coagulative necrosis was rare with PFA. Coagulative necrosis is not consistently noted with PFA,<sup>1</sup> and this rare finding could reflect a small amount of thermal injury with PFA, but this may also represent delayed healing of the MI itself, as coagulative necrosis is well described as part of the early and intermediate stages of MI repair.<sup>17–19</sup>

The finding of selective PFA effects on surviving myocytes within the scar and extending to the epicardial border of the scar is promising, as clinical ablation of ventricular arrhythmias often seeks to target or even 'homogenize' these tissues, which may be critical isthmuses for re-entry.<sup>20</sup> Conversely, the inability to selectively target viable myocytes within a chronic MI scar is a well-described limitation of RF,<sup>9,20</sup> in which resistive heating may be limited by a 'shunting' of current away from higher-impedance myocytes by lower impedance scar, and myocytes may be insulated from conductive heating by surrounding intra-scar fat and collagen. Pulsed-field ablation, which does not markedly rely on resistive or conductive heating, may help overcome these issues and benefit from the well-known lower electrical impedance of scar tissue, which may provide more effective conduction of PFA effects to the surviving myocytes.<sup>21,22</sup> To this point, a recent direct comparison of PFA (using multi-electrode linear and basket ablation catheters) with focal RF within a chronic MI scar found PFA lesions to be deeper ( $6.1 \pm 1.7$  mm) than RF ( $3.8 \pm 1.7$  mm) and comparable to the depths in our study ( $5.3 \pm 1.9$  mm).<sup>14</sup>

One limitation of our study is that we did not perform a direct comparison of PFA with RF in chronic MI scars and only provide indirect comparisons with the chronic MI RF studies discussed above.<sup>9,14</sup> However, we utilized multiple controls to support that contraction bands and myocytolysis of surviving myocytes were acute PFA findings (neither noted on control chronic MI scar without ablation) and that coagulative necrosis was rare (when compared with high-intensity ultrasound thermal ablation of chronic MI scar). Our data were generated with a proprietary PFA waveform at a single dose and, as with all

PFA studies, the results are not generalizable across platforms with different pulsed durations, pulsed repetition frequencies, voltage/amplitudes, pulses per packet, number of packets, and electrode size/configuration. However, we did perform our study with a 3.5 mm irrigated, CF-sensing catheter comparable to those used clinically, which should provide some degree of generalizability. Finally, our study did not assess the chronic evolution of PFA performed in/around chronic MI scars, as this would have required a 'double survival' pre-clinical study. Thus, it cannot be confirmed that the PFA effects (contraction bands and myocytolysis) of surviving myocytes within the scar will definitively lead to irreversible scar homogenization. However, these pathologic findings are well-known acute markers of eventual scar formation, both in studies of ablation and in those of MI.<sup>17–19</sup>

## Conclusion

PFA is able to generate ventricular lesions of significant depth, contiguous linear lesions without gaps, and selective ablation of surviving myocytes in and beyond the chronic MI scar via contraction band necrosis and myocytolysis (but rare coagulative necrosis). Translation to clinical use for catheter ablation of ventricular arrhythmias will require an assessment of chronic evolution and 'durability' of PFA lesions made in/around the myocardial scar.

## Supplementary material

Supplementary material is available at *Europace* online.

## Funding

This study was partially supported by an investigator-initiated grant from Galaxy Medical. B.N. is separately supported by K08-HL138156 and R01-HL160712 from the National Institutes of Health (NIH).

**Conflict of interest:** This study was partially supported by an investigator-initiated research grant from Galaxy Medical. B.N. also holds investigator-initiated research grants from Siemens Medical and Biosense Webster; he receives consulting fees from Edwards Lifesciences, Boston Scientific, and Biosense Webster. Q.C. and K.C. were employees of Galaxy at the time of this study. All remaining authors have no conflicts of interest.

## Data availability

Data are stored in a secure research server at OHSU and can be accessed upon request by investigators contacting the corresponding author.

## References

- Verma A, Asivatham SJ, Deneke T, Castelli Q, Neal RE II. Primer on pulsed electrical field ablation: understanding the benefits and limitations. *Circ Arrhythm Electrophysiol* 2021;**14**:e010086.
- Wittkamp FHM, van Es R, Neven K. Electroporation and its relevance for cardiac catheter ablation. *JACC Clin Electrophysiol* 2018;**4**:977–86.
- Reddy VY, Anic A, Koruth J, Petru J, Funasako M, Minami K et al. Pulsed field ablation in patients with persistent atrial fibrillation. *J Am Coll Cardiol* 2020;**76**:1068–80.
- Reddy VY, Dukkipati SR, Neuzil P, Anic A, Petru J, Funasako M et al. Pulsed field ablation of paroxysmal atrial fibrillation: 1-year outcomes of IMPULSE, PEFCAT, and PEFCAT II. *JACC Clin Electrophysiol* 2021;**7**:614–27.
- Koruth JS, Kuroki K, Iwasawa J, Viswanathan R, Brose R, Buck ED et al. Endocardial ventricular pulsed field ablation: a proof-of-concept preclinical evaluation. *Europace* 2020;**22**:434–9.
- Neven K, van Driel V, van Wessel H, van Es R, Doevendans PA, Wittkamp F. Epicardial linear electroporation ablation and lesion size. *Heart Rhythm* 2014;**11**:1465–70.
- Sugrue A, Vaidya VR, Livia C, Padmanabhan D, Abudan A, Isath A et al. Feasibility of selective cardiac ventricular electroporation. *PLoS One* 2020;**15**:e0229214.
- Yavin HD, Higuchi K, Sroubek J, Younis A, Zilberman I, Anter E. Pulsed-field ablation in ventricular myocardium using a focal catheter: the impact of application repetition on lesion dimensions. *Circ Arrhythm Electrophysiol* 2021;**14**:e010375.
- Barkagan M, Leshem E, Shapira-Daniels A, Sroubek J, Buxton AE, Saffitz JE et al. Histopathological characterization of radiofrequency ablation in ventricular scar tissue. *JACC Clin Electrophysiol* 2019;**5**:920–31.
- Nazer B, Walters TE, Duggirala S, Gerstenfeld EP. Feasibility of rapid linear-endocardial and epicardial ventricular ablation using an irrigated multipolar radiofrequency ablation catheter. *Circ Arrhythm Electrophysiol* 2017;**10**:e004760.
- Tanaka Y, Genet M, Chuan Lee L, Martin AJ, Sievers R, Gerstenfeld EP. Utility of high-resolution electroanatomic mapping of the left ventricle using a multispline basket catheter in a swine model of chronic myocardial infarction. *Heart Rhythm* 2015;**12**:144–54.
- Nazer B, Giraud D, Zhao Y, Hodovan J, Elman MR, Masri A et al. High-intensity ultrasound catheter ablation achieves deep mid-myocardial lesions in vivo. *Heart Rhythm* 2021;**18**:623–31.
- Nazer B, Salgaonkar V, Diederich CJ, Jones PD, Duggirala S, Tanaka Y et al. Epicardial catheter ablation using high-intensity ultrasound: validation in a swine model. *Circ Arrhythm Electrophysiol* 2015;**8**:1491–7.
- Im SI, Higuchi S, Lee A, Stillson C, Buck E, Morrow B et al. Pulsed field ablation of left ventricular myocardium in a swine infarct model. *JACC Clin Electrophysiol* 2022;**8**:722–31.
- Marchlinski FE, Callans DJ, Gottlieb CD, Zado E. Linear ablation lesions for control of unmappable ventricular tachycardia in patients with ischemic and nonischemic cardiomyopathy. *Circulation* 2000;**101**:1288–96.
- Yokoyama K, Nakagawa H, Shah DC, Lambert H, Leo G, Aebly N et al. Novel contact force sensor incorporated in irrigated radiofrequency ablation catheter predicts lesion size and incidence of steam pop and thrombus. *Circ Arrhythm Electrophysiol* 2008;**1**:354–62.
- Munz MR, Faria MA, Monteiro JR, Aguas AP, Amorim MJ. Surgical porcine myocardial infarction model through permanent coronary occlusion. *Comp Med* 2011;**61**:445–52.
- Miyazaki S, Fujiwara H, Onodera T, Kihara Y, Matsuda M, Wu DJ et al. Quantitative analysis of contraction band and coagulation necrosis after ischemia and reperfusion in the porcine heart. *Circulation* 1987;**75**:1074–82.
- Pasotti M, Prati F, Arbustini E. The pathology of myocardial infarction in the pre- and post-interventional era. *Heart* 2006;**92**:1552–6.
- Di Biase L, Burkhardt JD, Lakkireddy D, Carbucicchio C, Mohanty S, Mohanty P et al. Ablation of stable VTs versus substrate ablation in ischemic cardiomyopathy: the VISTA randomized multicenter trial. *J Am Coll Cardiol* 2015;**66**:2872–82.
- Amoros-Figueras G, Jorge E, Alonso-Martin C, Traver D, Ballesta M, Bragos R et al. Endocardial infarct scar recognition by myocardial electrical impedance is not influenced by changes in cardiac activation sequence. *Heart Rhythm* 2018;**15**:589–96.
- Schwartzman D, Chang I, Michele JJ, Mirotznic MS, Foster KR. Electrical impedance properties of normal and chronically infarcted left ventricular myocardium. *J Interv Card Electrophysiol* 1999;**3**:213–24.